Photography Enhancement Based on the Fusion of Tone and Color Mappings in Adaptive Local Region

Te-Hsun Wang, Chih-Wei Fang, Ming-Chian Sung, and Jenn-Jier James Lien*, *Member, IEEE*

EDICS: TEC-RST Restoration and Enhancement

ABSTRACT

Existing tone reproduction schemes are generally based on a single image and are therefore unable to accurately recover the local details and colors of scene since the limited available information. Accordingly, the proposed tone reproduction system utilizes two images with different exposures (one low and one high) to capture the local detail and color information of low- and high-luminance regions of scene, respectively. The adaptive local region of each pixel is developed in order to appropriately reveal the details and maintain the overall impression of scene. Our system implements the local tone mapping and color mapping based on the adaptive local region by taking the lowly-exposed image as the basis and referencing the information of highly-exposed image. The local tone mapping compresses the luminance range in the image and enhances the local contrast to reveal the details, while the local color mapping maps the precise color information from the highly-exposed image to the lowly-exposed image. Finally, a fusion process is proposed to mix the local tone mapping and local color mapping results to produce the output image. A multi-resolution approach is also developed to reduce time cost. The experimental results confirm that the system generates realistic reproductions of HDR scenes.

Index Terms**—**Tone reproduction, high dynamic range, local tone mapping, local color mapping.

Department of Computer Science and Information Engineering, National Cheng Kung University, Taiwan 70101, R.O.C.
Email: {dsw_1216, nat, qwer, jjlien*}@csie.ncku.edu.tw Phone: +886-6-2757575 ext. 62540 Fax: +886-6-2747076

I. INTRODUCTION

Tone reproduction schemes are essential in resolving the problem which occurs when attempting to reproduce real-world scenes characterized by a wide luminance range on display devices with only a limited capability. Consider, for example, the lowly-exposed image (I_L) shown in Fig. 1.a. In capturing this real-world scene, the brighter regions are well-exposed at the expense of the darker regions of the image, which are under-exposed. As a result, the details in the brighter regions are accurately recorded, but the recorded color information in the darker regions is noisy or lost. Fig. 1.b illustrates the opposite case of a highly-exposed image (I_H). In this case, the darker regions of the scene are well-exposed, but the brighter regions are overexposed. Thus, the colors of the objects in the darker regions of the image are faithfully reproduced, but the bright regions appear washed out (i.e. the color fades to white). Consequently, when attempting to accurately reproduce a real-world scene, it is impossible to capture the full dynamic range of the scene using a single image acquired with a fixed exposure setting. For example, increasing the luminance linearly in I_L may result in the brighter regions being over-exposed and the darker regions washed out (see Fig. 1.c). Similarly, reducing the luminance linearly in I_H not only results in the darker regions being under-exposed, but also fails to reveal the details in the brighter regions of the image since these details were not recorded by the camera when taking the original image (see Fig. 1.d). Thus, some form of tone mapping scheme is required to map (or compress) the high dynamic range (HDR) luminance of the real world scene to the low dynamic range (LDR) luminance capabilities of the display device in order to accurately reproduce the realistic image (see Fig. 1.e).

A. Related work

There are various proposals for uniform (i.e. global) tone mapping methods such as: [22], [24]. However, some works like [3] and [19] found that while these global tone mapping methods are reasonably successful in resolving the tone reproduction problem and avoiding visual halo artifacts, the resulting images tend to lose the local details (blur) of the scene. Therefore, non-uniform (i.e. local) tone mapping methods are proposed to provide a good tone reproduction performance and preserve the finer details of the original scene. Non-uniform tone reproduction methods are usually implemented by computing the local adaptation luminance (locally-averaged luminance) to simulate the local adaptation effect of human's visual system. When computing the local adaptation luminance, the size of local region is a crucial consideration since the overly-small region is too small to reveal sufficient details and maintain the perceptual impression of the scene, while the overly-large region tends to improperly emphasize the local details. The local region size is generally determined in accordance with some form of local contrast measure. Various techniques have been proposed for deriving the locally-averaged luminance using multi-scale Gaussian filters. For example, Reinhard *et al*. [19] chose a center-surround function [2] implemented by subtracting two Gaussian blurred images, and Ashikhmin [1] adopt similar scheme to determine the scales of Gaussian filters. Some researchers have proposed the use of anisotropic diffusion methods as a means of computing the locally-averaged luminance of a scene. For example, Tumblin *et al*. [21] used low curvature image simplifier (LCIS), a partial differential equation inspired by anisotropic diffusion, to blur the HDR image whilst preserving the sharpness of the edges. Other researchers, [5] and [6], have implemented anisotropic diffusion schemes in the form of bilateral filters in which two weights are assigned in the spatial and range domains, respectively, in order to explain the intensity differences between each pixel and its neighbors. Different from above, another pixel-wise approach presented by Fattal *et al.* [8] using a gradient domain local tone mapping scheme that emphasized attenuating large gradients and solved a Poisson equation to recover the luminance. It is found that the local region size determined using the pixel-wise methods presented in [1], [5], [6], [19], [21], [22] and [24] is generally too local (i.e. too small) to reveal sufficient details. In general, however, the pixel-wise approaches described above focus primarily on the local adaptation aspects of the tone reproduction problem, but tend to overlook the need to maintain the consistency in the luminance contrast (perceptual impression) of the scene. Although this problem was addressed by the piece-wise method presented by Chen *et al*. [3], the system tended to improperly emphasize the local details with the larger local regions. Meylan *et al.* [13] proposed a surround-based Retinex method for HDR rendering that used an adaptive filter whose shape follows the high-contrast edges in the image to reduce halo artifacts. A color transformation based on principal component analysis (PCA) was applied to the RGB channels of the input image to obtain an image which took the first component of the PCA as the luminance channel and the other two as the chrominance. The local adaption was performed using a surround-based Retinex method applied to the luminance channel only. PCA provided orthogonality among channels thus reduces the chromatic changes caused by processing of the luminance. However, the brighter regions may over-exposed after rendering if the regions in the original input image were well-exposed (i.e. lowly-exposed image).

As described above, the dynamic range of most real-world scenes is so great that attempts to record the scene invariably result in some regions of the image being over-exposed and some being under-exposed. As a result, the details of the real-world scene within these regions of the image are lost. In addition, luminance compression techniques based on a single image with a fixed exposure level inevitably fail to reproduce the perceptual qualities of the original scene. The literature contains many examples of image processing applications in which multiple input images are used to increase the amount of information available. Typical applications include noise removal using flash and no-flash pairs [7], [15]; color transfer [18], [20]; color transfer for image deblurring using highly-exposed and lowly-exposed pairs [11]; and gray scale image colorization [12]. Goshtasby [9] showed that the additional information provided by multiple images with different exposures was also beneficial in enhancing the performance of HDR reduction schemes. Similarly, Debevec *et al*. [4] produced HDR images of real scenes by recovering the response function of an imaging process from serial different exposed pictures of the static scene. However, the schemes presented in [4] and [9] both assume that any change in the value of each individual pixel from one image to the next is the result only of a change in the exposure. As a result, the use of a fixed tripod is essential in acquiring images, and thus the practicality of both methods is somewhat limited.

B. Proposed method

To resolve the problems described above, this study develops a novel tone reproduction system which takes two input images with different exposure conditions as inputs. Modern digital cameras invariably feature a built-in exposure bracketing capability which allows a series of images to be obtained at different exposure levels via a single depression of the shutter release mechanism. This functionality is exploited to capture two images of a high contrast scene with different levels of exposure (lowly-exposed, I_L and highly-exposed, I_H) such that the details and color of the scene can be accurately reproduced. Although the two images have different exposure levels and may blur or slightly shift caused by camera shake, the coherence nevertheless exists in their color statistics and spatial constraints [11] since they are taken successively of the same scene. The basic principle of the tone reproduction system developed in this study is to exploit these coherences to reproduce the details and color of the scene in a realistic fashion. Since the high luminance regions of a scene are characterized by a greater light range than the darker regions, the details in these regions of the scene are not easily recorded by a low dynamic range device, and thus highly-exposed images generally contain one or more saturated high luminance regions. Therefore, the proposed system takes the lowly-exposed image (I_L) as its basis, and refines this image using the tone and color information associated with the highly-exposed image (I_H).

Fig. 2 shows the flowchart of proposed system. Section II describes the developed appropriate local region size (adaptive local region), represents as the range of neighboring pixels which belong to the similar luminance, calculated for later processes. Section III.A shows that the local tone mapping module commences by using a global tone mapping technique to increase the luminance of the low-luminance regions of I_L. The overall luminance range of the image is then compressed by applying a local tone mapping scheme to reveal details of scene. Section III.B shows the local color mapping module which is developed for overcoming the overly compressed of luminance range and the considerable noise of darker regions. The global color characteristic of I_H on I_L is initially imposed using a global color mapping scheme and the precise color of each pixel is then refined using a local color mapping method. A fusion process is applied to combine the local tone mapping result (I_T) and the local color mapping result (I_C) to create the final display image (I_D) as described in Section III.C. In addition, the Section IV interprets the developed multi-resolution approach which is used to reduce the time cost of the proposed tone reproduction system.

II. LOCAL REGION DETERMINATION

When viewing a real-world scene, the human vision system subconsciously compensates for differences in the local luminance intensities of different regions of the scene when interpreting its contents. In order to perform the biological function, this study commences by determining the local region of each pixel. In the proposed approach, a histogram-based segmentation process is applied to group the luminance values of the various pixels in the image into a small number of discrete intervals. The local region radius of each pixel is then determined using an iteration map derived from a morphological erosion operation. In practice, the local region radius defines the range of neighboring pixels which belong to the same luminance interval and should therefore be processed in an equivalent manner.

A. Histogram-based luminance segmentation

Since the light range in the high luminance regions of a scene is greater than that in the darker regions, the details within these regions are generally lost when recording the scene using a low dynamic range (LDR) device. In the proposed tone reproduction system, the problem of luminance differences within an image is addressed by grouping the luminance values of all the pixels in the lowly-exposed image (I_L) into a range of contiguous intervals using a histogram-based segmentation approach. It has been shown that the entropy theorem provides a suitable means of determining the optimal threshold value when separating the darker and brighter regions of an image [16]. According to this theorem, the threshold value t is computed in such a way as to maximize the sum of the entropies of the two distributions (i.e. the dark and bright regions). Given the probabilities P_d^i of dark pixels (i.e. a luminance value $\leq t$) with luminance i and P_b^i of bright pixels (i.e. a luminance value $\geq t$) with luminance i, t is computed in accordance with

$$Entropy = \arg\max_t \left(-\sum_{i=0}^{t} p_d^i \log p_d^i - \sum_{i=t}^{255} p_b^i \log p_b^i\right) \tag{1}$$

Fig. 3.a illustrates the example of segmenting a typical luminance histogram (L_L) into four subintervals defined by [L_{min}, L_{low}], [L_{low}, L_{middle}], [L_{middle}, L_{high}] and [L_{high}, L_{max}], respectively. Adopting a dichotomy approach, the segmentation procedure is repeated three times in order to yield three threshold values, i.e. L_{low}, L_{middle} and L_{high}; of which L_{middle} lies in the interval [L_{min}, L_{max}] obtained in the first pass, L_{low} lies in the interval [L_{min}, L_{middle}] obtained in the second pass, and L_{high} lies in the

interval [L_{middle}, L_{max}] obtained in the final pass. The values of L_{low}, L_{middle}, and L_{high} provide the means to determine whether the luminance value of any particular pixel belongs to the low luminance, lower-middle luminance, higher-middle luminance or high-luminance interval of the histogram.

In the proposed tone reproduction system, each of these four intervals is further partitioned into two intervals, i.e. the segmentation procedure is repeated until the luminance histogram is partitioned into eight subintervals. And each pixel whose luminance falls within a particular range is treated identically to all other pixels having a luminance within the same range. In segmenting the lowly-exposed image, it is invariably found that there exist some small regions caused by noisy pixels. In general, however, these regions are too small to reveal details and thus in the proposed system, they are removed by using a median filter following the segmentation process. Fig. 3.b presents the typical results of the histogram segmentation process.

B. Iteration map creation for local region determination

Having segmented the lowly-exposed image into several regions in accordance with the luminance values of the individual pixels, a circular local region $R_{x,y}$ is then determined for each pixel (x, y). The radius of each local region, R, is determined by performing an iterative morphological erosion operation within each luminance region, and creating an iteration map to record the iteration number at which each pixel is eroded. Clearly, for pixels located closer to the boundary of any luminance region, the corresponding iteration value is lower, while for those pixels located closer to the center of the luminance region, the iteration value is higher. For each pixel (x, y), the radius of the circular local region is then set equal to the value of the iteration map in the corresponding pixel position. Fig. 4.a and 4.b illustrate a typical morphological erosion operation and the corresponding iteration map, respectively, while Fig. 4.c superimposes typical circular local regions determined using the process described above on the corresponding luminance histogram-segmented image.

III. TONE REPRODUCTION SYSTEM

A. Luminance (details): pixel-wise local tone mapping module

Fig. 5 illustrates the basic concept of the proposed local tone mapping module. As shown, the module comprises a luminance scaling (i.e. global tone mapping) function to brighten the darker regions of the image and a local tone mapping function to suppress the resulting over-exposed, brighter regions of the image. The tone mapping module commences by applying a luminance scaling process to the lowly-exposed image, I_L, to generate an initial middle-gray tone image. Since I_L contains under-exposed darker regions, it is necessary to apply a greater scaling effect to the darker regions to brighten the concealed details by Eqs. (2) and (3).

$$\overline{L}_k = \exp\left(\frac{1}{N}\sum_{x,y}\log(\delta + L_k(x,y))\right),\quad L_k \in \{L_L, L_H\} \tag{2}$$

$$L(x,y) = \alpha\frac{\overline{L}_H}{\overline{L}_L}L_L(x,y) \tag{3}$$

where $\overline{L}_L$ and $\overline{L}_H$ are the log-average luminance (referred to as the key values in [10], [22] and [23]) of I_L and I_H, respectively, and are used to objectively measure whether the scene has a low-gray, middle-gray or high-gray tone. Furthermore, in Eq. (2), N is the total number of pixels in I_L or I_H and δ is a very small value used to avoid the unreasonable log 0. Meanwhile, in Eq. (3), $L_L(x, y)$ is the luminance value of pixel (x, y) in I_L and is normalized to the interval [0, 1]. Then, the scale of integral α is assigned a value of α =5 to ensure compatibility with the total compression range of the global tone mapping function used in the subsequent local tone mapping process (see Fig. 6). By applying Eqs. (2) and (3), the luminance L_L of the lowly-exposed image is scaled to an overall luminance L. Fig. 7 presents the luminance images of two typical lowly- and highly-exposed images (i.e. L_L and L_H, respectively) and shows the corresponding globally-scaled luminance image (i.e. L).

Following the global tone mapping process, a local tone mapping process is performed which mimics the human vision system by locally adapting luminance differences so as to compress the luminance of the brighter regions. Reinhard *et al.* [19] presented a simple non-uniform local tone mapping technique for compressing the luminance range of a scene such that all of its luminance values fall within the interval [0, 1]:

$$L_T = \frac{L}{1+V} = H \times V' = \left(\frac{L}{V}\right)\times\left(\frac{V}{1+V}\right) \tag{4}$$

This tone mapping method is to extract the details of scene, and then, to compress the local adaptation luminance only. By Eq. (4), the relationship between the globally-scaled luminance L and the local adaptation luminance *V* causes the brighter pixels in the darker regions of the image to become brighter ($L>1+V$) and the darker pixels in the brighter regions of the image to become darker ($L<1+V$). The luminance compression term *V'* is the local adaptation luminance *V* compressed using the global tone mapping function also proposed by Reinhard *et al.* [19].

In the proposed system, it modulates both the local contrast and the luminance compression by extracting the detailed term (denoted as *H*, see Fig. 8.a) and the local adaptation luminance compression term (denoted as *V'*, see Fig. 8.b) with the following formula proposed by Chen *et al.* [3]:

$$L_T(L,V,\rho,\varphi) = \underbrace{\left(\frac{L}{V}\right)^{\rho}}_{H} \times \underbrace{\left(\frac{V}{1+V}\right)^{\varphi}}_{V'} \tag{5}$$

The parameters ρ and φ in Eq. (5) are assigned values in the range $0<\rho<2$ and $0<\varphi\leqq 1$, respectively in accordance with Chen *et al.* [3] proposed. The parameter ρ controls the degree of sharpness that the larger value generates the sharper result; however, the jagged edge (aliasing) problem may arise in over sharp reproduction. The parameter φ controls the degree of luminance compression, that is, as the value reduced, the luminance values of the darker regions are scaled into a larger display range. In the following reproduction results of proposed system, the parameters ρ=1.2 and φ=1 are applied based on our experience.

Since the radius of the circular local region $R_{x,y}$ has already been determined for each pixel (x, y) in Section II.B, the value of the local adaptation luminance *V* for pixel (x, y) can be obtained simply from the geometry and luminance variations of the neighboring pixels by convoluting the luminance values in the local region using a series of weighted masks (a generalized version of bilateral filtering proposed by Chen *et al.* [3]), i.e.

$$V(x,y) = \frac{1}{Z_{x,y}}\left(\sum_{(i,j\in R_{x,y})} L(i,j)G_{x,y}(i,j)K_{x,y}(i,j)\right) \tag{6}$$

$$\mathrm{G}_{x,y}(i,j) = \exp\left(-((i-x)^2+(j-y)^2)/2\sigma_s^{\,2}\right) \tag{7}$$

$$\mathrm{K}_{x,y}(i,j) = \exp\left(-(L(i,j)-L(x,y))^2/2\sigma_r^{\,2}\right) \tag{8}$$

$$Z_{x,y} = \sum_{(i,j\in R_{x,y})} G_{x,y}(i,j)K_{x,y}(i,j) \tag{9}$$

The significance of each neighboring pixel (i, j) when performing this convolution process is evaluated using $G_{x,y}$ and $K_{x,y}$, which are Gaussian weights corresponding to the spatial distance between pixels (x, y) and (i, j) and the difference in luminance of the two pixels, respectively. In the proposed local tone mapping module, σ_s in Eq. (7) is set equal to 4% of the image size while σ_r in Eq. (8) is specified as σ_r =0.4. And $Z_{x,y}$ in Eq. (9) is a normalization term. The result of local adaptation luminance is shown in Fig. 8.c. The local tone mapping module finishes by refining the original lowly-exposed image I_L into a tone-mapped image I_T by scaling the pixel value of each *RGB* channel according to the luminance change ratio, obtained by dividing the output luminance L_T by the input scaled luminance L, i.e.

$$I_T{}^k = I_L{}^k \times \frac{L_T}{L}, \qquad k \in \{R,G,B\} \tag{10}$$

Fig. 9 illustrates the effects of parameters α in Eq. (3) and ρ and φ in Eq. (5) with the local mapping results. In Fig. 9.a, 9.b and 9.c, the α is varied with fixed ρ and φ to show different degrees of luminance scaling (i.e. global tone mapping) in the fixed display range. Fig. 9.d, 9.e and 9.f show the different degrees of sharpness with varied ρ and fixed α and φ. In g and h, the different display ranges for dark region are varied with φ. In the following experimental results, the parameters $\alpha = 5, \rho = 1.2$ and $\varphi = 1$ are assigned for general situation. The $\rho = 1.2$ is assigned instead of larger value to prevent the jagged edge (aliasing) problem.

B. Color: pixel-wise local color mapping module

The described local tone mapping module refines the luminance values of the pixels and enhances the local contrast to reveal the details in the lowly-exposed image. However, the consistency in the luminance contrast of scene sometimes may lose since the luminance range is overly compressed. In addition, the image may contain imprecise *RGB* color information as the image exposed based on the brighter region of the scene and the dark regions inevitably under-exposed. That is, the imprecise color information may be recorded when the darker regions of the scene are so dark, and it makes the darker regions contain considerable noise. To resolve this problem, the local color mapping module proposed in this study applies a global color mapping scheme initially to impose the color characteristics of the source image I_H on the target image I_L, and then performs the refined procedure, a pixel-wise local color mapping operation, to acquire the precise color.

Reinhard *et al.* [18] proposed the following simple statistical analysis method (global color mapping operation used in this paper) for imposing the color characteristics of I_H on the I_L:

$$I_L^{k'}(x,y) = g\left(I_L^k(x,y)\right) = \mu_H^k + \frac{\sigma_H^k}{\sigma_L^k}(I_L^k(x,y) - \mu_L^k), \quad k \in \{l,\alpha,\beta\} \tag{11}$$

where $I_L(x, y)$ is the color value of pixel (x, y) in each $\ell\alpha\beta$ channel [17] of the lowly-exposed image, μ_L and σ_L are the mean and standard deviation of the color value of I_L, respectively, and μ_H and σ_H are the mean and standard deviation of the color value in I_H, respectively. The global color transfer process is performed on each $\ell\alpha\beta$ channel and the results are then converted back to the *RGB* color space to obtain the preliminary global color transfer result I_L'. The $\ell\alpha\beta$ color space is adopted since the correlation of the axes in $\ell\alpha\beta$ color space is much lower than that of those in other color spaces. Fig. 10 presents a typical target image I_L' and the original source image I_H.

However, the global color transfer process fails to obtain the precise local color information when the source or target image contains many different color regions since it cannot distinguish the different statistics and therefore mixes some of the regions up. Moreover, the image pair (i.e. I_L and I_H) may not be perfectly aligned, i.e. the pixels in one image may not be located in precisely the same positions as their counterparts in the second image. Fig. 11.a and 11.b present two typical examples in which the scenes recorded in the two images are blurred or slightly shifted due to camera shake. Clearly, in this situation, the pixel in the lowly-exposed image can not be modulated directly using the detailed and color information of the pixel in the corresponding position in the highly-exposed image. Hence, the proposed system applies a further pixel-wise local color mapping process in the *RGB* color domain based on the geometry and luminance variations of the neighboring pixels in order to get the true local color for pixel (x, y) from pixel (i^*, j^*) in I_H in the local color mapping region $S_{x,y}$, i.e.

$$(i^*, j^*) = \underset{(i,j)\in S_{x,y}}{\operatorname{argmax}} \left(\exp(-\frac{(I_L'(x,y) - I_H(i,j))^2}{2\sigma^2}) \times \exp(-\frac{((i-x)^2 + (j-y)^2)}{2\sigma^2}) \right) \tag{12}$$

where σ is assigned a value equal to half the iteration value of pixel (x, y). In addition, $S_{x,y}$ is the local color mapping region for each pixel (x, y), and varies inversely in size with the value of pixel $(x,$

y) in the iteration map. As described in Section II.B, if pixel (x, y) has a small iteration value, it must be located near the region boundary. Clearly, the pixels in the target image located near a boundary are particularly susceptible to color transfer errors as a result of motion blurring or camera-shake. Therefore, in order to get the precise color information for pixels with a smaller iteration value, it is necessary to search for the appropriate color within a larger local color mapping region (see upper circle in Fig. 12). By contrast, the color of pixels with a larger iteration value is less sensitive to the effects of motion blurring or camera shake. As a result, the color information of the corresponding pixels in I_H is sufficiently precise, and thus the search for the appropriate color information can be performed within a smaller color mapping region (see lower circle in Fig. 12). Having obtained the value of (i*, j*) from Eq. (12), the color value of pixel $I_L'(x, y)$ in the lowly-exposed globally color-mapped image is replaced by that of pixel $I_H(i^*, j^*)$ in the source image in order to construct the final local mapping result I_C.

C. Fusion of local tone mapping and local color mapping results

Fig. 13 summarizes the basic properties of the tone-mapped and color-mapped images, i.e. I_T and I_C, respectively. It is observed that the properties of the two images are complementary to one another. For example, the high-luminance regions in I_T are well-exposed, while those in I_L are over-exposed. Similarly, I_C is characterized by precise color information and low noise, whereas I_T has saturated color regions and noisy dark regions. Accordingly, the tone reproduction system presented in this study performs a fusion process to blend the local tone mapping result I_T and local color mapping result I_C to create the final display result I_D, i.e.

$$I_D = \alpha_{x,y} I_T + (1 - \alpha_{x,y}) I_C \tag{13}$$

$$\text{where } \alpha_{x,y} = \begin{cases} \dfrac{\beta_{x,y}}{1 + \exp\left(-2 \dfrac{L_L(x,y) - L_{middle}}{|L_{middle} - L_{low}|} \right)} & \text{if } L_L(x,y) < L_{middle} \\ \dfrac{\beta_{x,y}}{1 + \exp\left(-2 \dfrac{L_L(x,y) - L_{middle}}{|L_{middle} - L_{high}|} \right)} & \text{otherwise.} \end{cases} \tag{14}$$

Fig. 14 illustrates the double-sigmoid function [14] used to generate the weights $\alpha_{x,y}$ in Eq. (13).

This function provides a virtually linear fusion over the interval [L_{low}, L_{high}] and a non-linear fusion over the intervals [L_{min}, L_{low}] and [L_{high}, L_{max}], respectively. In the dark regions of the image, the pixels in I_C are assigned a higher weight during the fusion process in order to generate a more precise color effect and to reduce the noise in I_T. By contrast, in the bright regions of the image, the pixels in I_T are assigned a greater weight in order to compensate for the color and details in the saturated regions of I_C. Since the pixels located near the region boundary may be affected by the camera shake problem, the confidences of the local color mapping for these pixels are reduced in the fusion process. Parameter $\beta_{x,y}$ in Eq. (14) is assigned in the range $1 \geqq \beta_{x,y} \geqq 0.5$ to control the color appearance of the fused image I_D for these pixels that the value of $\beta_{x,y}$ varies inversely with the value of pixel (x, y) in the iteration map ($e_{x,y}$), i.e.

$$\beta_{x,y} = 0.5 \times (1 + \frac{M - e_{x,y}}{M - 1}) \qquad (15)$$

where M is the maximal value of the iteration map.

Fig. 15.a and 15.b present typical examples of the local tone mapping result I_T and local color mapping result I_C, respectively. The corresponding reproduction result, I_D, is shown in Fig. 15.c. The Fig. 15.d, 15.e and 15.f are the enlarged portions of Fig. 15.a, 15.b and 15.c, respectively. It is found that I_T succeeds in revealing the details, but the noise is also revealed and fails in maintaining the consistency in the impression of the scene. Contrary to I_T, I_C shows no noise and maintains the consistency in the impression, however, the detail is not revealed. The result I_D is reproduced to give a good balance in the complementary properties.

IV. Acceleration Using Multi-Resolution Approach

The time cost are consuming in executing the morphological erosion process (see Section II.B), the local luminance adaptation process (see Section III.A) and the color searching process (see Section III.B) with large image size or with large local region size. Accordingly, as described in the following sections, the tone reproduction system proposed in this study is implemented using a multi-resolution approach to improve the time cost. The concept of proposed multi-resolution approach is to generate the initial results by executing the original complex operator at the coarse resolution, and then to refine the results at the fine resolution. The coarse-to-fine processing speeds the proposed system by decreasing the amount of pixels which are necessary to perform the complex computing operators.

Before the bottom level is achieved by down-sampling, the histogram-based segmentation is performed in advance. The morphological eroding operation is then performed to determine the local region for each pixel at the bottom level. Also, the processes of local adaptation luminance computation and local color mapping are applied at the bottom level. Afterward, the up-sampling is implemented and the adjustment mechanism is applied to revise the imprecise value caused by interpolation operation in the up-sampling process. We will describe how to apply the multiple-resolution approach in our local tone mapping module and local color mapping module in the Section 4.A and 4.B, respectively.

A. Implementation of pixel-wise local tone mapping using multi-resolution approach

Fig. 16 presents a flowchart showing the multi-resolution implementation of the local luminance adaptation process in the local tone mapping module. As shown, the multi-resolution approach takes the globally-scaled luminance image L^0 as the input and performs $l-1$ down-sampling operations in order to produce a cascaded series of scaled luminance images L^i (i =0~$l-1$). Having completed the down-sampling process, the bottom level image, i.e. L^{l-1}, is taken as an input to compute the corresponding local adaptation luminance V^{l-1} using the method described in Section III.A. Up-sampling is then performed on V^{l-1}. However, the interpolation operation performed in the up-sampling process results in an imprecise local adaptation luminance value for each pixel. Thus, since L^i contains the original luminance information of level i, the value of L^i is used at each level to adjust the up-sampling result V^i in accordance with the following linear formulation:

$$V^{i}{}'(x,y)=\frac{\sum_{\Delta x=-k}^{k}\sum_{\Delta y=-k}^{k}(1-W^{i})L^{i}(x+\Delta x,y+\Delta y)+W^{i}V^{i}(x,y)}{\sum_{\Delta x=-k}^{k}\sum_{\Delta y=-k}^{k}1},\quad i=l-2\sim 0 \tag{16}$$

where values of W^i=0.5 and k=1 are specified in the proposed system. As a result, the overall global impression of the original image is retained in the up-sampling process. The visual effect of this adjustment process is shown in Fig. 17. Finally, the value of $V^{0\prime}$ is taken as V in Eq. (9) and is used to carry out the local tone mapping process on a pixel-by-pixel basis.

B. Implementation of pixel-wise local color mapping using multi-resolution approach

Fig. 18 presents a flowchart showing the multi-resolution implementation of the local color mapping module. The basic principle of the multi-resolution approach is to use a larger local color mapping region $S_{x,y}$ to search for an appropriate mapping color at the lower levels of the down-sampled cascade and to progressively reduce the size of the local color mapping region $S_{x,y}$ for adjusting at the higher levels. Accordingly, the mapping process commences by conducting the local color mapping procedure described in Section III.B at the bottom level of the cascade, i.e. l-1, in order to find the local mapping color and the mapping pair relating the position pair $P^{l\text{-}1}\{(x, y), (x^*, y^*)\}$ of pixel (x, y) in I_L' with the corresponding mapping pixel in I_H. By using the recorded position pairs as the index, the target mapping position at level l-2 can be estimated. The estimated target position is then taken as the search center, and a smaller local color mapping region $S_{x,y}$ is used to search for a new mapping color and a new mapping pair $P^{l\text{-}2}\{(x, y), (x^*, y^*)\}$ for level l-2.

V. Experimental Results

To confirm the feasibility of the proposed tone reproduction system, a series of experiments were performed on a PC with an Intel Pentium 4 (3.2GHz) processor. The execution time was found to vary with the number and size of the segmentation regions. However, in general, the results showed that a 640×480 image could be processed within an average of 8 seconds. TABLE I summarizes the running times of the proposed method when applied to the “window scene” used throughout this study for illustration purposes. TABLE II indicates the overall running times of the proposed system when implemented using a multi-resolution approach with different down-sampling levels. It is evident that the multi-resolution approach yields a significant reduction in the overall computational time. TABLE III presents an itemized breakdown of the running time of the proposed system when implemented with 3 levels. The tables show that although the proposed multi-resolution approach doesn’t reduce the computational complexity of proposed tone reproduction algorithm, the used coarse-to-fine processing strategy is still useful in reducing the running time cost. As shown, the multi-resolution approach reduces the overall time duration from around 7.31 seconds to just 2.28 seconds, representing a time saving of around 69%.

The proposed system is inspired by Jia *et al*. [11] which properly formulating color statistics and spatial constraints by using their proposed Bayesian framework with input image pair, I_L and I_H. Fig. 19 shows the input image pair, the mapping result of [11] and our result for comparison. It is found that the input image I_H (Fig. 19.b) is a little bit blurred; but, two methods are successful in revealing the detail. However, the result of Jia *et al*. [11] (Fig. 19.c) appears washed out (i.e. the colors fade to white as luminance increase).

When implementing the local tone reproduction methods presented in the literature, the size of the local region is a crucial factor. Fig. 20 compares the local regions estimated by the schemes presented in [19] and [3] with that obtained using the method presented in this study. And the I_L of input image pair of proposed system is used as input to [19] and [3]. It can be seen that the local region derived using the method proposed by Reinhard *et al*. [19] may be too small to reveal sufficient local details. Conversely, the region estimated using the region-wise method presented in [3] is not always adaptive for each pixel in the region and may therefore cause unnatural emphasis on details. However, the morphological erosion method proposed in the current study enables the derivation of a more adaptive local region size (see Fig. 20.c). Fig. 21 compares the local tone mapping results obtained using the proposed system with those obtained using the methods presented in [19] and [3], respectively. The tone mapping method presented in [19] fails to reveal sufficient details of low luminance region and maintain the perceptual impression of scene as Fig. 21.d and 21.f shown, respectively. Furthermore, the unnatural emphasis case of the region-wise method proposed in [3] is evident in the slightly unnatural color appearance (Fig. 21.h and 21.i). Instead of maintaining the details of high luminance region as Fig. 21.f, the Fig. 21.i and 21.l prefer to reveal sufficient details of low luminance region and maintain the perceptual impression of scene.

Fig. 22 shows some other results of color transfer [18], photographic tone reproduction [19], piece-wise tone reproduction [3], and our method. It is found that the color transfer [18] fails in high dynamic range scene while the other three methods are practicable. And the tone reproduction [19] sometimes may not reveal the detail of the dark regions (Fig. 22.b and 22.j). In addition, the piece-wise tone reproduction [3] shows the impressive ability of revealing sufficient details. However, the appearing colors are too saturated that makes the mapping results unnatural.

Figs. 23~26 present typical results obtained using the proposed tone reproduction system. Fig. 23 shows that besides having the ability to process HDR images, the system can also deal successfully with LDR images. The colors fade to white when exposed to light in the I_H (Fig.23.b) are recovered in I_D (Fig.23.e). Meanwhile, the results presented in Fig. 24 confirm the ability of overcoming the camera-shake (i.e. blurring) problem between image pairs when transferring the true pixel colors from I_H to I_L in the proposed local color mapping process. Fig. 25 demonstrates that the proposed method successfully preserves the details within the brighter regions of the image even when the real-world scene is characterized by an extremely high dynamic range. Finally, Fig. 26.e shows that the proposed system has reduced the noise within the darker regions of the local tone mapping result I_T by fusing I_T with the non-noisy local color mapping result I_C as far as possible. The fusion result I_D (Fig.26.e) shows that the details of dark region have been revealed and the “color fade” of I_H have also been recovered. However, since the low color resolution within the dark region (color information lost) of I_L causes serious noise of I_T, the performance of the proposed system is limited that the noise can’t be removed completely.

VI. CONCLUSIONS

Tone reproduction is essential when attempting to reproduce real-world HDR scenes on LDR display devices. However, most tone reproduction techniques fail to accurately reveal the color and details of HDR scenes. Accordingly, this study has developed a tone reproduction system in which two images of the real-world scene are acquired successively at different exposures (one low and one high) and are supplied to an automatic local adaptation mechanism which takes account of both the color statistics and the spatial constraints between the two images in order to accurately reveal the color and detailed information of the original scene.

Since the human vision system subconsciously adapts the local luminance differences within a scene when observing its contents. In this study, this biological function is mimicked by applying an adaptive local region concept to each pixel such that all pixels of a similar luminance are treated in an equivalent manner. In the proposed approach, the pixels within the lowly-exposed image are grouped into a small number of discrete intervals using a histogram-based segmentation process based upon entropy theory. The local region radius of each pixel is then evaluated from an iteration map derived from a morphological erosion process. The proposed tone reproduction system comprises two pixel-wise modules, namely a local tone mapping module and a local color mapping module. The tone mapping module brightens the darker regions, compresses the luminance range to suppress the resulting over-exposed and enhances the local contrast in order to reveal the details of the image. However, the consistency in impression of the scene may lose since the luminance range is overly compressed and saturated color may appear in the local tone mapping result. Hence, the color mapping module maps the true color information from the highly-exposed image to the lowly-exposed image is proposed. Then, a fusion process based on a double-sigmoid weighting function is then applied to fuse the local tone mapping results and the local color mapping results to produce a satisfactory display result. The experimental results have shown that the proposed system has the ability not only to process HDR images, but also to resolve the tone reproduction problems posed by LDR images, camera shake images, and noisy images, respectively. In addition, it has been shown that by implementing the proposed tone reproduction system using a multi-resolution approach with three down-sampling levels, the overall computational time can be reduced by the order of 69%.

REFERENCES

[1] M. Ashikhmin, "A Tone Mapping Algorithm for High Contrast Images," *13th Eurographics*, pp.145–156, 2002.

[2] F.J.J. Blommaert and J.B. Martens, "An Object-Oriented Model for Brightness Perception," *Spatial Vision*, Vol.5, No.1, pp.15-41, 1990.

[3] H.T. Chen, T.L. Liu, and C.S. Fuh, "Tone Reproduction: A Perspective from luminance-Driven Perceptual Grouping," *International Journal of Computer Vision*, Vol. 65, pp. 73-96, 2005.

[4] P.E. Debevec and J. Malik, "Recovering High Dynamic Range Radiance Maps from Photographs," *ACM SIGGRAPH*, pp. 369-378, 1997.

[5] J.M. DiCarlo and B.A. Wandell, "Rendering High Dynamic Range Images," *SPIE: Image Sensors*, Vol. 3965, pp. 392-401, 2000.

[6] F. Durand and J. Dorsey, "Fast Bilateral Filtering for the Display of High-Dynamic-Range Images," *ACM SIGGRAPH*,

pp. 257-266, 2002.

[7] E. Eisemann and F. Durand, "Flash Photography Enhancement via Intrinsic Relighting," *ACM Transactions on Graphics*, Vol. 23, No. 3, pp. 673-678, 2004.

[8] R. Fattal, D. Lischinski, and M. Werman, "Gradient Domain High Dynamic Range Compress," *ACM SIGGRAPH*, pp. 249-256, 2002.

[9] A.A. Goshtasby, "High Dynamic Range Reduction via Maximization of Image Information," http://www.cs.wright.edu/~agoshtas/hdr.html.

[10] J. Holm, "Photographic Tone and Colour Reproduction Goals," *CIE Expert Symposium '96 on Colour Standard for Image Technology*, pp. 51-56, 1996.

[11] J. Jia, J. Sun, C.K. Tang, and H.Y. Shum, "Bayesian Correction of Image Intensity with Spatial Consideration," *European Conference on Computer Vision*, Vol. 3, pp. 342-354, 2004.

[12] A. Levin, D. Lischinski, and Y. Weiss, "Colorization Using Optimization," *ACM Transactions on Graphics*, Vol. 23, No. 3, pp. 689-694, 2004.

[13] L. Meylan and S. Süsstrunk, "High Dynamic Range Image Rendering with a Retinex-Based Adaptive Filter," *IEEE Transactions on Image Processing*, Vol. 15, No. 9, pp. 2820-2830, 2006

[14] K. Nandakumar, "Integration of Multiple Cues in Biometric Systems," *Master Thesis, Dept. of Computer Science and Engineering*, *Michigan State Uni.,* 2005.

[15] G. Petschnigg, R. Szeliski, M. Agrawala, M. Choen, H. Hoppe, and K. Toyama, "Digital Photography with Flash and No-Flash Image Pairs," *ACM Transactions on Graphics*, Vol. 23, No. 3, pp. 664-672, 2004.

[16] A. Pardo and G. Sapiro, "Visualization of High Dynamic Range Images," *IEEE Transactions on Image Processing*, Vol. 12, No. 6, pp. 639-647, 2003.

[17] D.L. Ruderman, T.W. Chonin, and C.C. Chiao, "Statistic of Cone Responses to Natural Images: Implications for Visual Coding," *J. Optical Soc. Of America*, Vol. 15, No. 8, pp. 2036-2045, 1998.

[18] E. Reinhard, M. Ashikhmin, B. Gooch, and P. Shirley, "Color Transfer between Images," *IEEE Computer Graphics and Application*, Vol. 21, pp. 34-41, 2001.

[19] E. Reinhard, M. Stark, P. Shirley, and J. Ferwerda, "Photographic Tone Reproduction for Digital Images," *ACM SIGGRAPH*, pp. 267-276, 2002.

[20] Y.W. Tai, J. Jia and C.K. Tang, "Local Color Transfer via Probabilistic Segmentation by Expectation-Maximization," *Computer Vision and Pattern Recognition*, Vol. 1, pp. 747-754, 2005.

[21] J. Tumblin and G. Turk, "LCIS: A Boundary Hierarchy for Detail-Preserving Contrast Reduction," *ACM SIGGRAPH*, pp. 83-90, 1999.

[22] J. Tumblin and H. Rushmeier, "Tone Reproduction for Computer Generated Images," *IEEE Computer Graphics and Application*, Vol. 13, No. 6, pp. 42-48, 1993.

[23] G. Ward, "A Contrast-Based Scale Factor for Luminance Display," *Graphics Gems IV, P. Heckbert, Ed. Academic Press, Boston*, pp. 415-421, 1994.

[24] G. Ward, H.E. Rushmeuer, and C.D. Piatko, "A Visibility Matching Tone Reproduction Operator for High Dynamic

Range Scenes," *IEEE Transactions on Visualization and Computer Graphics,* Vol. 3, No. 4, pp. 291-306, 1997.

Authors:

Jenn-Jier James Lien (M'00) received his B.S. degree in biomedical engineering from Chung Yuan University, Taiwan, in 1989, and his M.S. and Ph.D. degrees in electrical engineering from Washington University, St. Louis, MO, and the University of Pittsburgh, Pittsburgh, PA, in 1993 and 1998, respectively. From 1995 to 1998, he was a research assistant at the Vision Autonomous Systems Center, Robotics Institute, Carnegie Mellon University, Pittsburgh, PA. From 1999 to 2002, he was a senior research scientist at L1-Ideneity (formerly Visionics), where he was also a project lead for the DARPA surveillance project on Human Identification at a Distance. In 2002, he joined the department of computer science and information engineering at National Cheng Kung University, Taiwan, as an associate professor and director of the robotics laboratory. He is currently a member of the technical committee of several IEEE conferences and a reviewer for a number of IEEE journals. His research interests include the computer vision and pattern recognition, human-computer interaction, surveillance and biometrics, and multimedia information analysis and retrieval.

Te-Hsun Wang received his B.S. degree in computer science and information engineering from Tam Kang University, Taipei, in 2002, and received his M.S. degree in computer science and information engineering from National Cheng Kung University, Taiwan, in 2004. Currently, he is a Ph.D. candidate in computer science and information engineering at National Cheng Kung University, Tainan, Taiwan. In addition to his current research into rigid and non-rigid motion separation for facial expression recognition, his interests lie in facial image analysis and synthesis, digital image processing, and computer vision.

Chih-Wei Fang received his B.S. degree in computer science and information engineering from National Cheng Kung University, Tainan, Taiwan, in 2004. He is a Ph.D. candidate in computer science and information engineering at National Cheng Kung University, Tainan, Taiwan. In addition to his current research into texture synthesis and image completion, his interests lie in image processing, computer vision and computer graphics.

Ming-Chian Sung received his B.S. degree in computer information science from National Chiao Tung University, in 2005, and received his M.S. degree in computer science and information engineering from National Cheng Kung University, Taiwan, in 2007. Currently he works at Garmin.

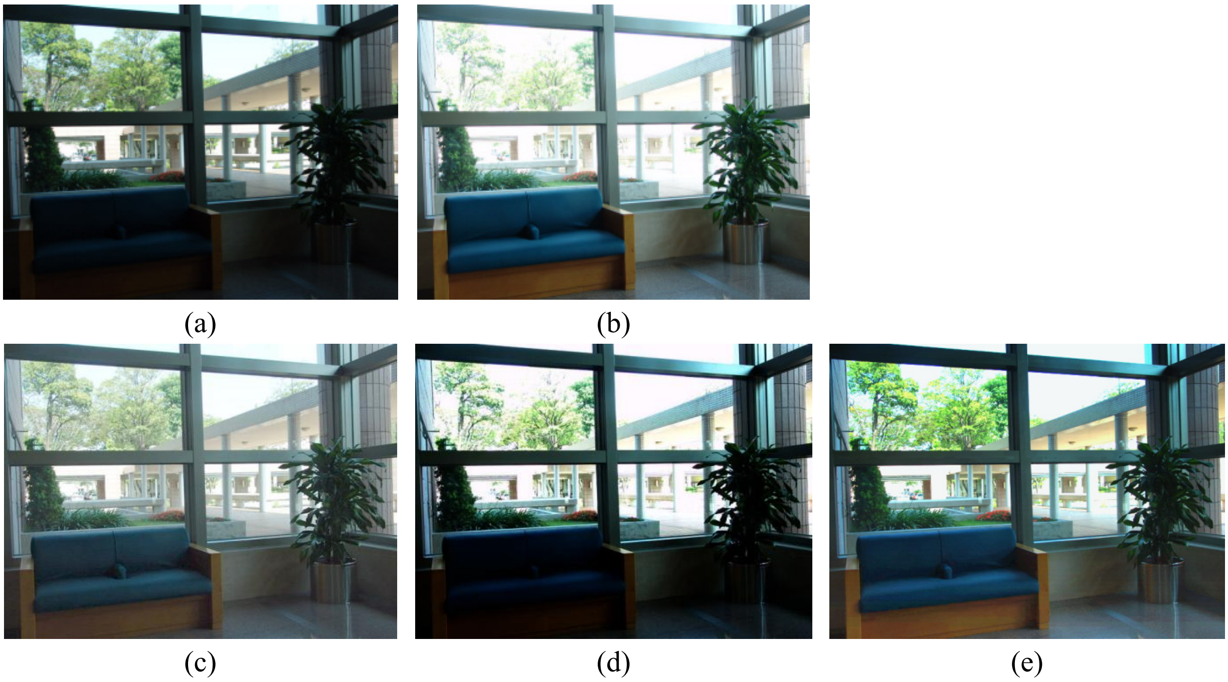

Fig. 1. Images for dynamic range and tone reproduction problem: (a) lowly-exposed image I_L. (b) highly-exposed image I_H. (c) Linear increase of luminance in I_L resulting in over-exposed brighter regions. (d) Linear decrease of luminance in I_H resulting in under-exposed dark regions. (e) Simulated HDR scene.

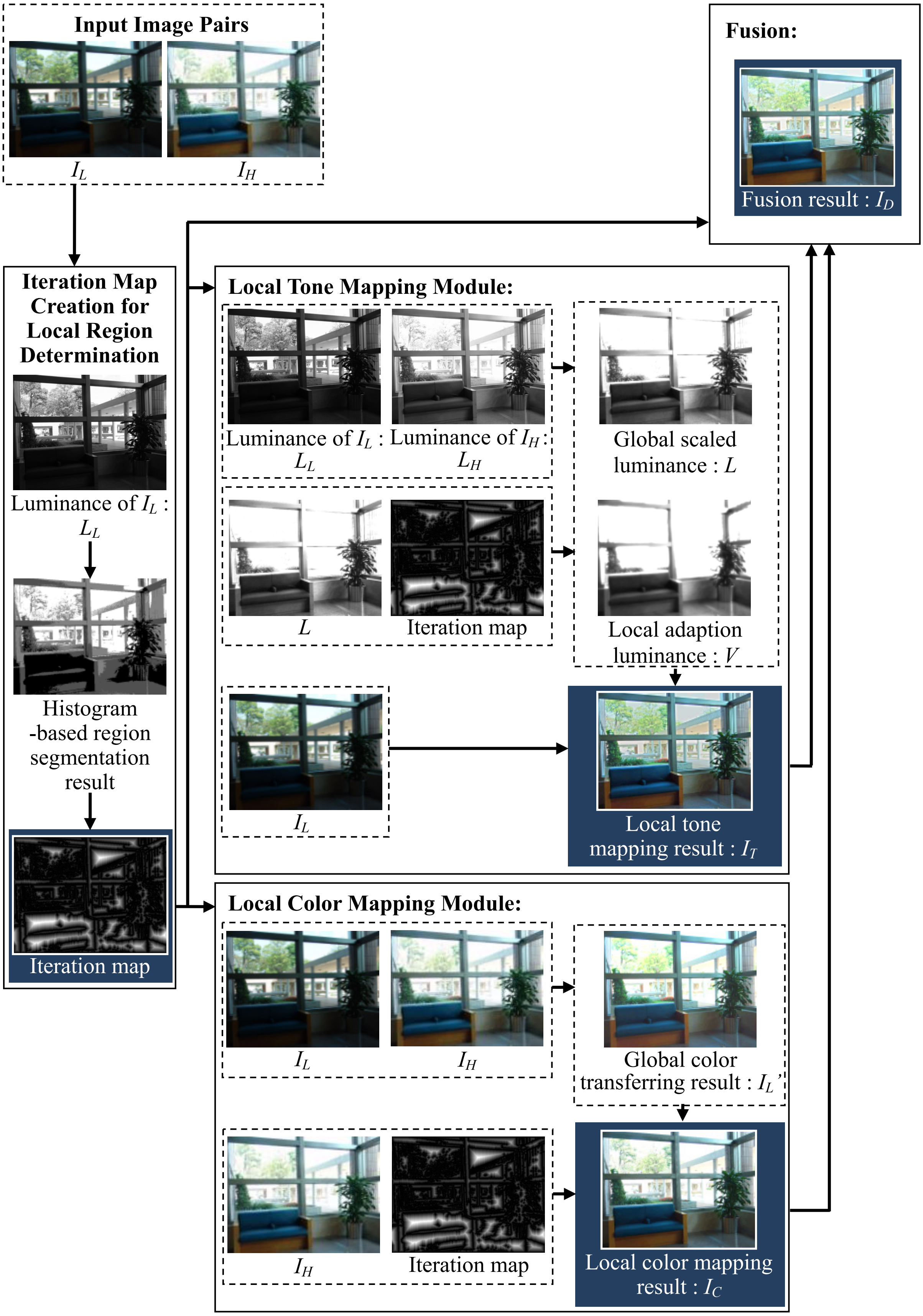

Fig. 2. Flowchart of proposed tone reproduction system.

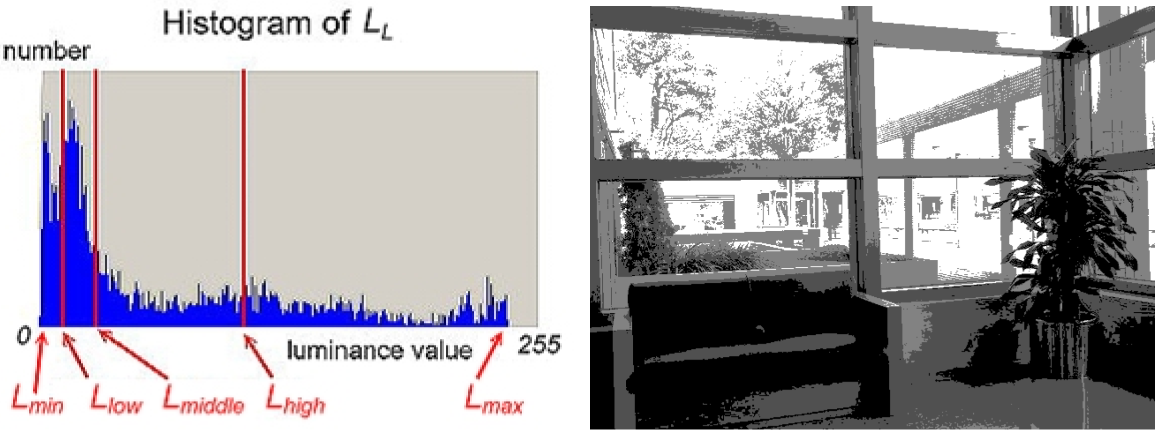

Fig. 3. Histogram-based region segmentation using entropy theorem. (a) Partitioning of luminance histogram L_L into 4 intervals in accordance with entropy theorem. (b) Histogram-based segmentation result with 8 intervals.

(a) (b) (c)

Fig. 4. Morphological erosion process and iteration map. (a) Snapshot of erosion operation after 3 iterations. (b) Iteration map of I_L, in which the brighter pixels indicate a larger iteration value. (c) Superimposition of typical local pixel regions and histogram-based segmented image.

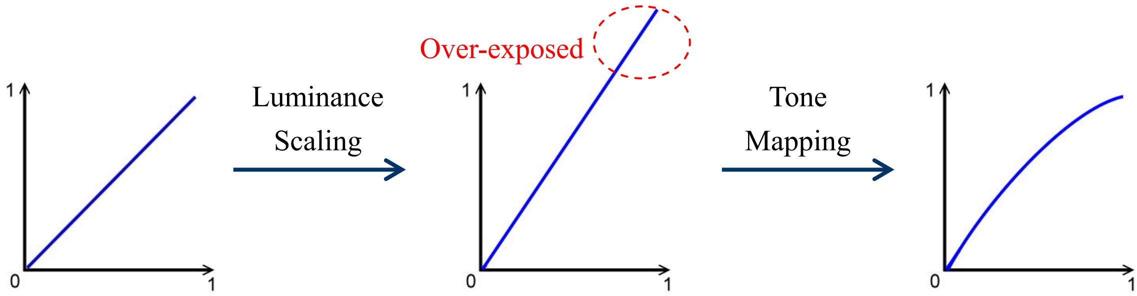

Fig. 5. Basic concept of local tone mapping module.

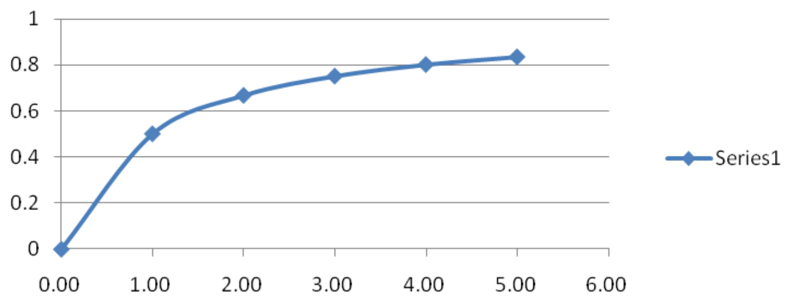

Fig. 6. Distribution of used luminance scaling (global tone mapping). Note that the x- and y-axes correspond to the normalized luminance values before and after modulation, respectively.

(a) (b) (c)

Fig. 7. Luminance scaling. (a) L_L: luminance image of lowly-exposed image I_L. (b) L_H: luminance image of highly-exposed image I_H. (c) Global scaled luminance image L.

(a) (b) (c)

Fig. 8. (a) Detailed term, H. (b) Local adaptation luminance compression term, V'. (c) Local adaptation luminance result V.

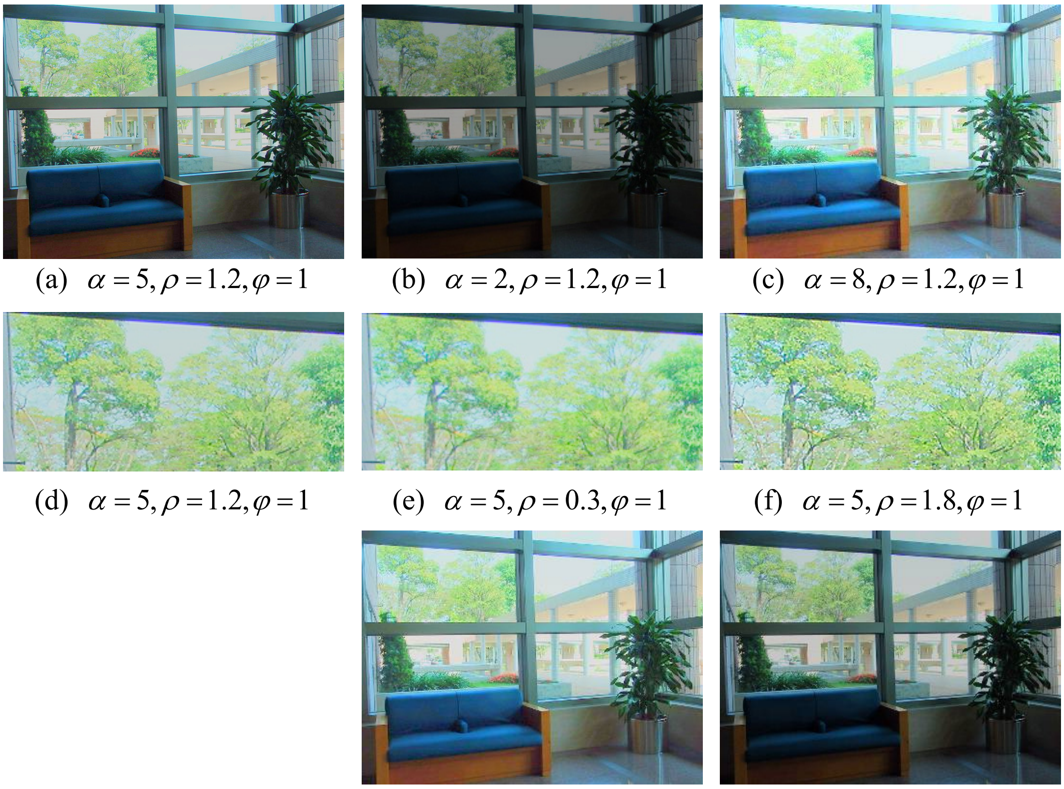

(a) $\alpha = 5, \rho = 1.2, \varphi = 1$ (b) $\alpha = 2, \rho = 1.2, \varphi = 1$ (c) $\alpha = 8, \rho = 1.2, \varphi = 1$

(d) $\alpha = 5, \rho = 1.2, \varphi = 1$ (e) $\alpha = 5, \rho = 0.3, \varphi = 1$ (f) $\alpha = 5, \rho = 1.8, \varphi = 1$

(g) $\alpha = 5, \rho = 1, \varphi = 0.7$ (h) $\alpha = 5, \rho = 1, \varphi = 1.3$

Fig. 9. Local tone mapping results with different parameters. (a), (b) and (c) change the α with fixed ρ and φ. (d), (e), and (f) change the ρ with fixed α and φ. (a), (g) and (h) change the φ with fixed α and ρ.

Fig. 10. Comparison of target image I_L' with source image I_H. (a) Global color transfer result I_L'. (b) Source image I_H.

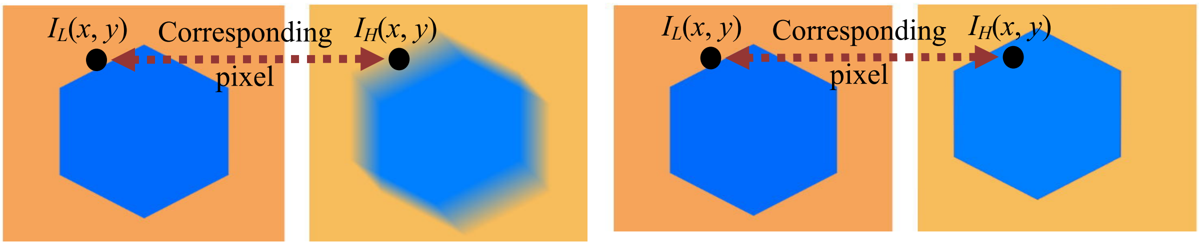

Fig. 11. Defective image pairs due to camera shake. (a) Blurred. (b) Slightly shifted.

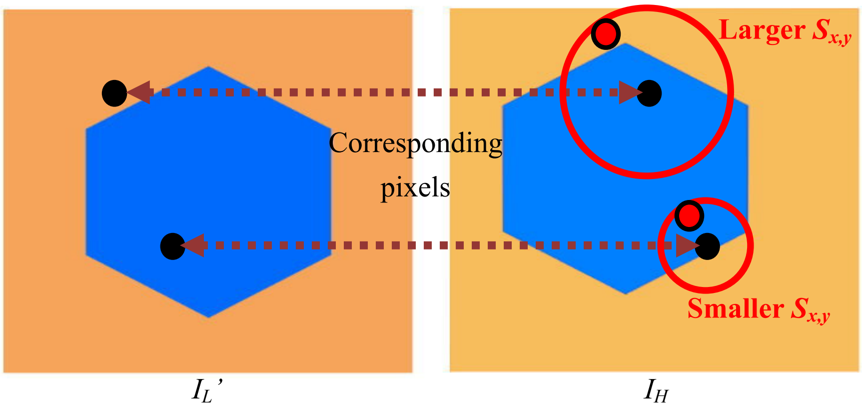

Fig. 12. Local color mapping region $S_{x,y}$. Note that the size of $S_{x,y}$ is inversely proportional to the value of pixel (x, y) in the iteration map. The black pixels represent the I_L'(x, y) and corresponding pixel I_H(x, y), while the red pixels represent the pixels found via the local color mapping scheme given Eq. (12).

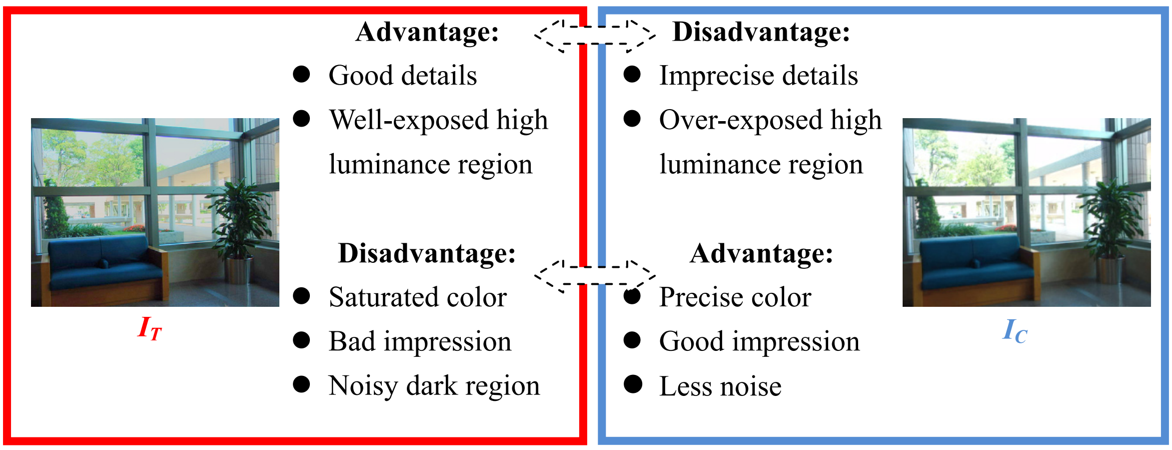

Fig. 13. Complementary properties of local tone mapping and local color mapping modules.

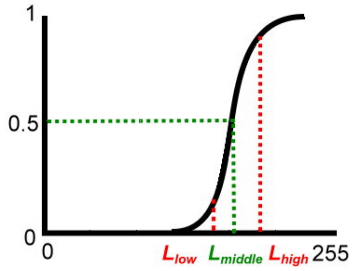

Fig. 14. Distribution of double-sigmoid weighting function.

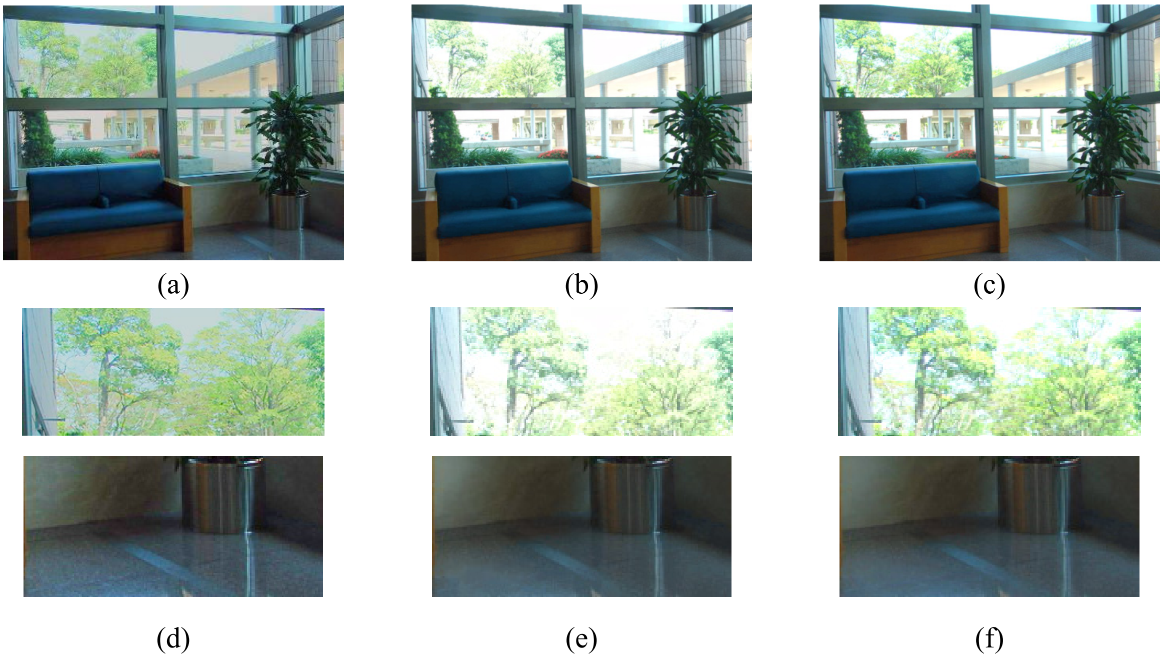

Fig. 15. Typical fusion results. (a) Local tone mapping result I_T. (b) Local color mapping result I_C. (c) Fusion result I_D. (d) Enlarged portions of I_T. (e) Enlarged portions of I_C. (f) Enlarged portions of I_D.

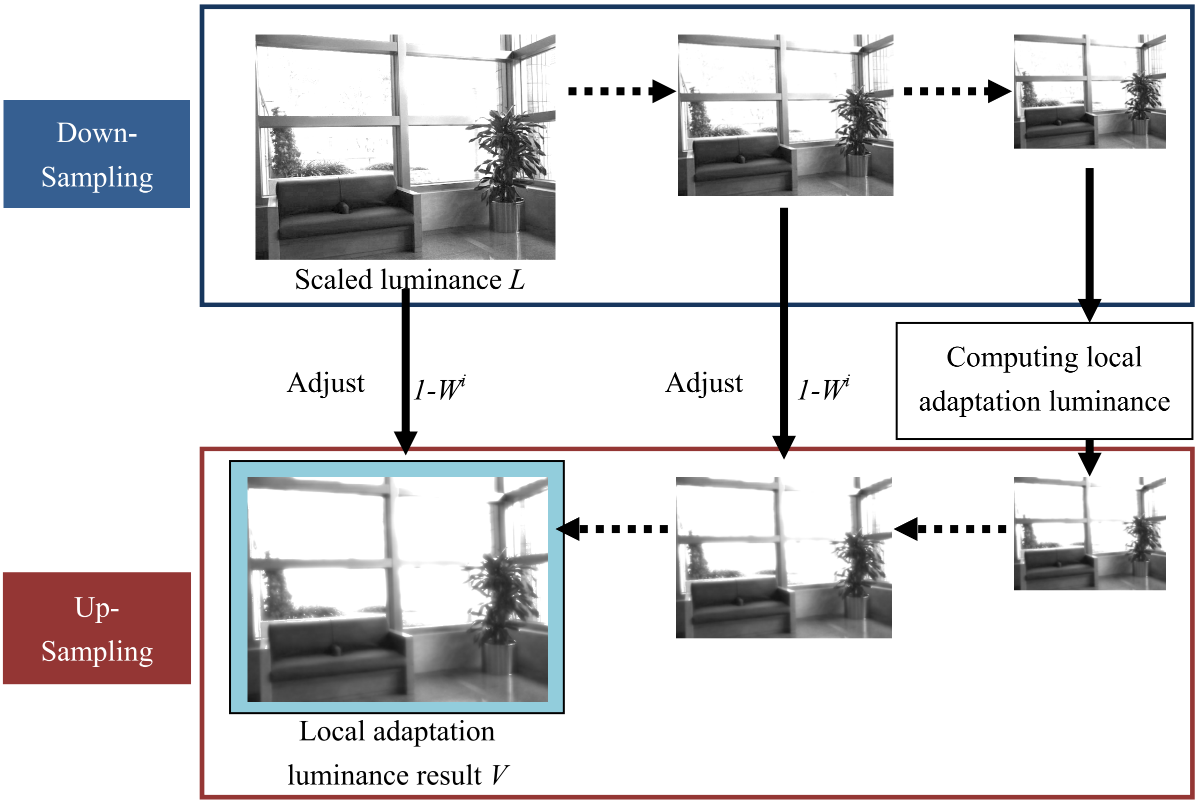

Fig. 16. Flowchart showing implementation of local luminance adaptation scheme using multi-resolution approach.

(a) (b)

Fig. 17. (a) Local tone mapping result without adjustment by *L*. (b) Local tone mapping result with adjustment by *L*.

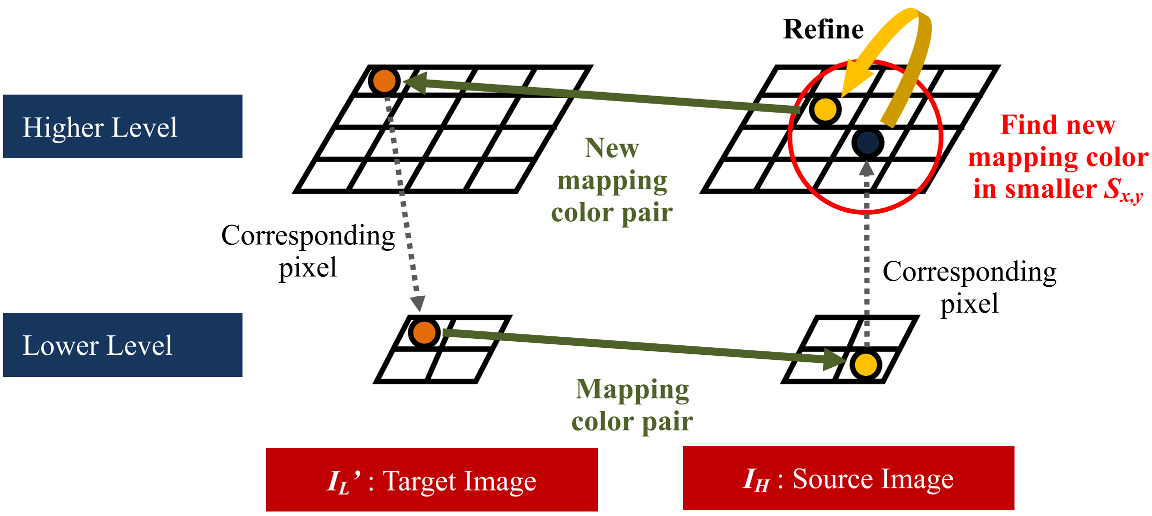

Fig. 18. Schematic illustration showing revision of local color mapping result after up-sampling.

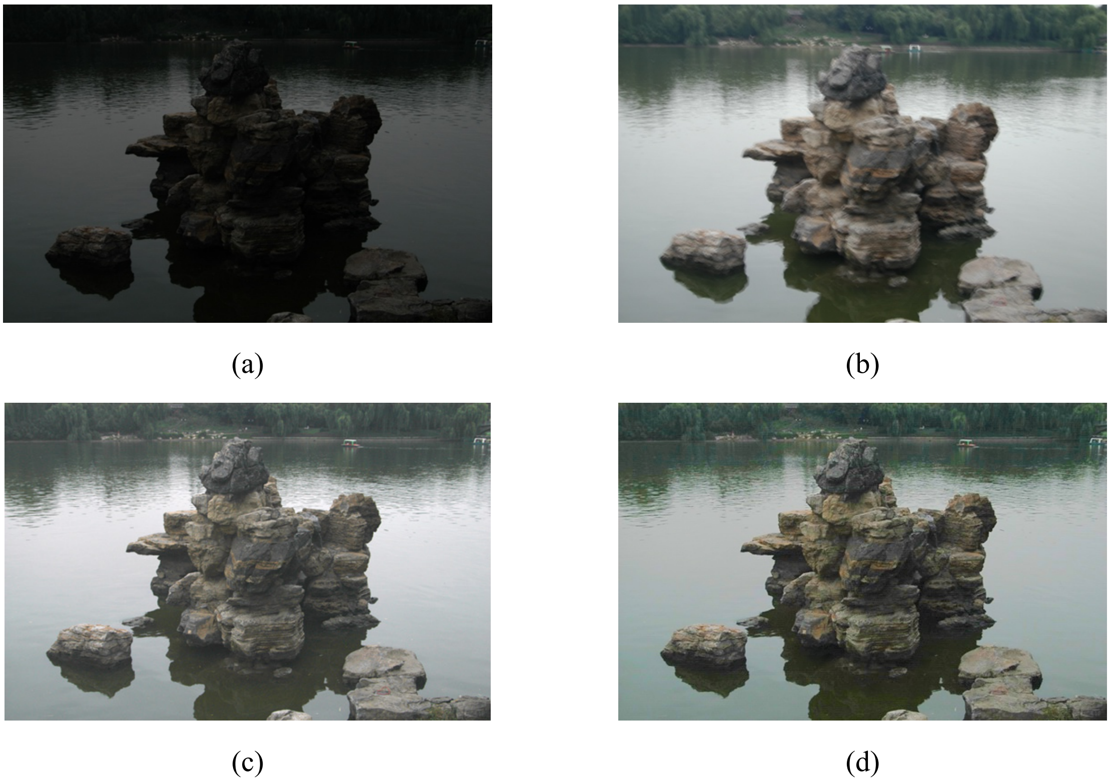

Fig. 19. Comparison of Jia *et al*. [11] and our method. (a) Input I_L. (b) Input I_H. (c) Result of Jia *et al*. [11]. (d) Our result.

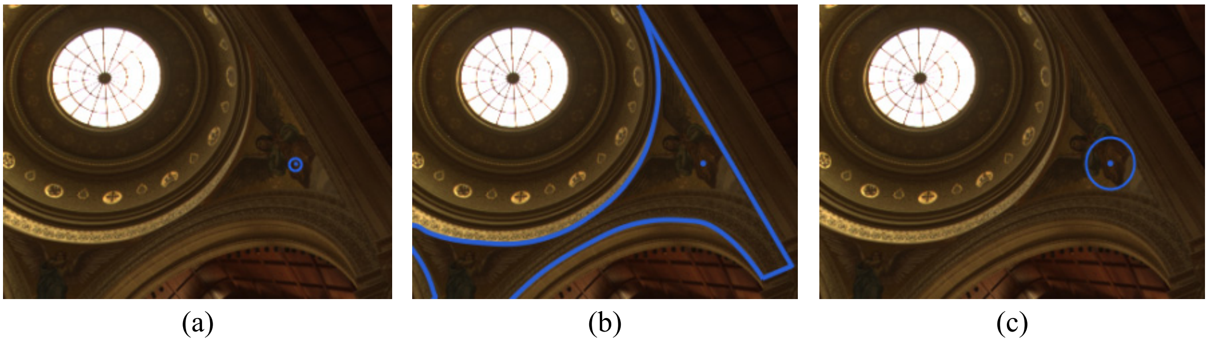

Fig. 20. Comparison of local regions determined by different methods. (a) Local region obtained using method proposed by Reinhard *et al*. [19]. (b) Local region identified by piece-wise method [3]. (c) Local region obtained using proposed morphological erosion method.

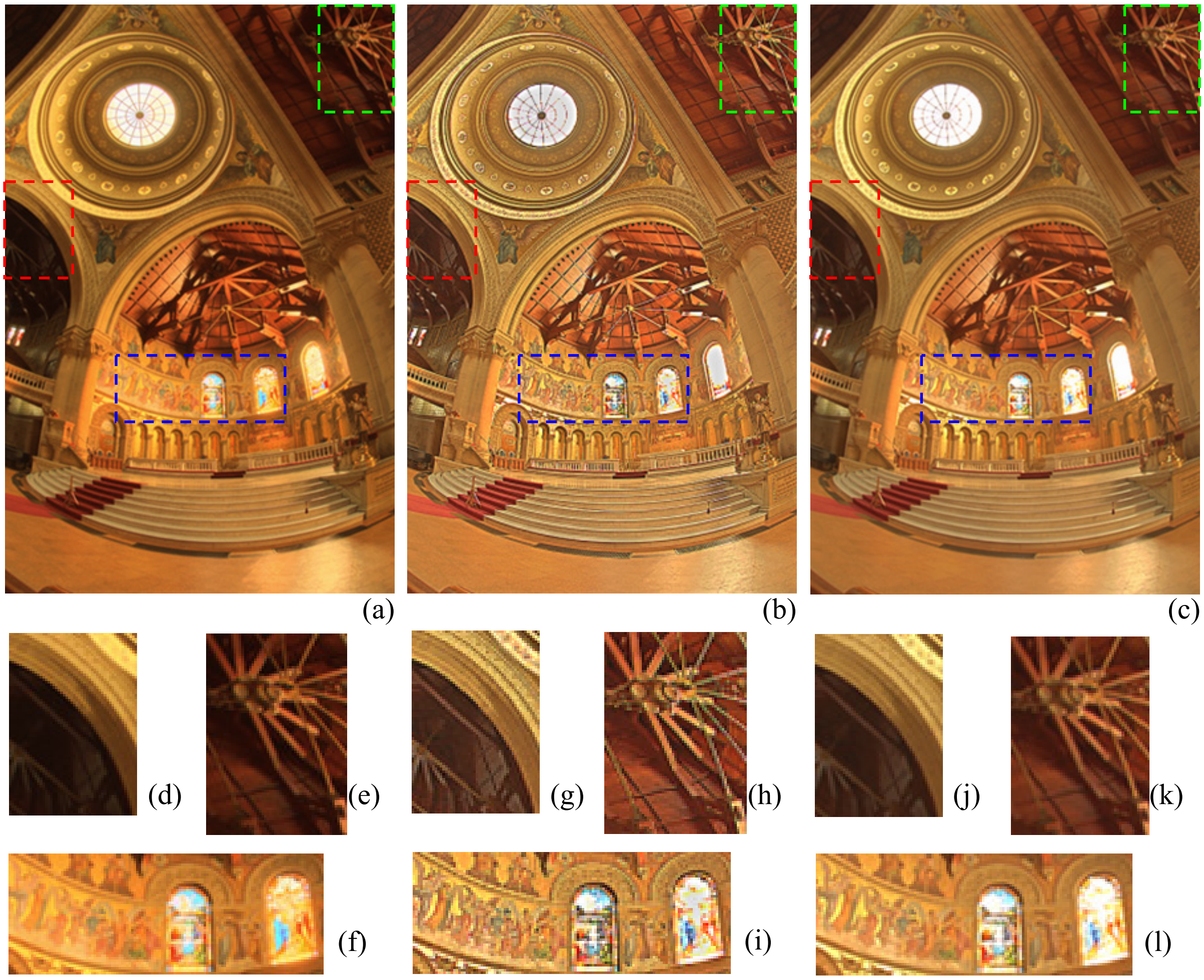

Fig. 21. Comparison of different tone mapping results. (a) Result obtained using method proposed by Reinhard *et al*. [19]. (b) Result obtained using piece-wise method [3]. (c) Result obtained using proposed method. (d),(e),(f) Enlarged portions of (a). (g),(h),(i) Enlarged portions of (b). (j),(k),(l) Enlarged portions of (c).

(a) [18] (b) [19] (c) [3] (d) Our method

(e) [18] (f) [19] (g) [3] (h) Our method

(i) [18] (j) [19] (k) [3] (l) Our method

(m) [18] (n) [19] (o) [3] (p) Our method

Fig. 22. Comparison of different methods: From left to right, color transfer [18], photographic tone reproduction [19], piece-wise tone reproduction [3], and our method.

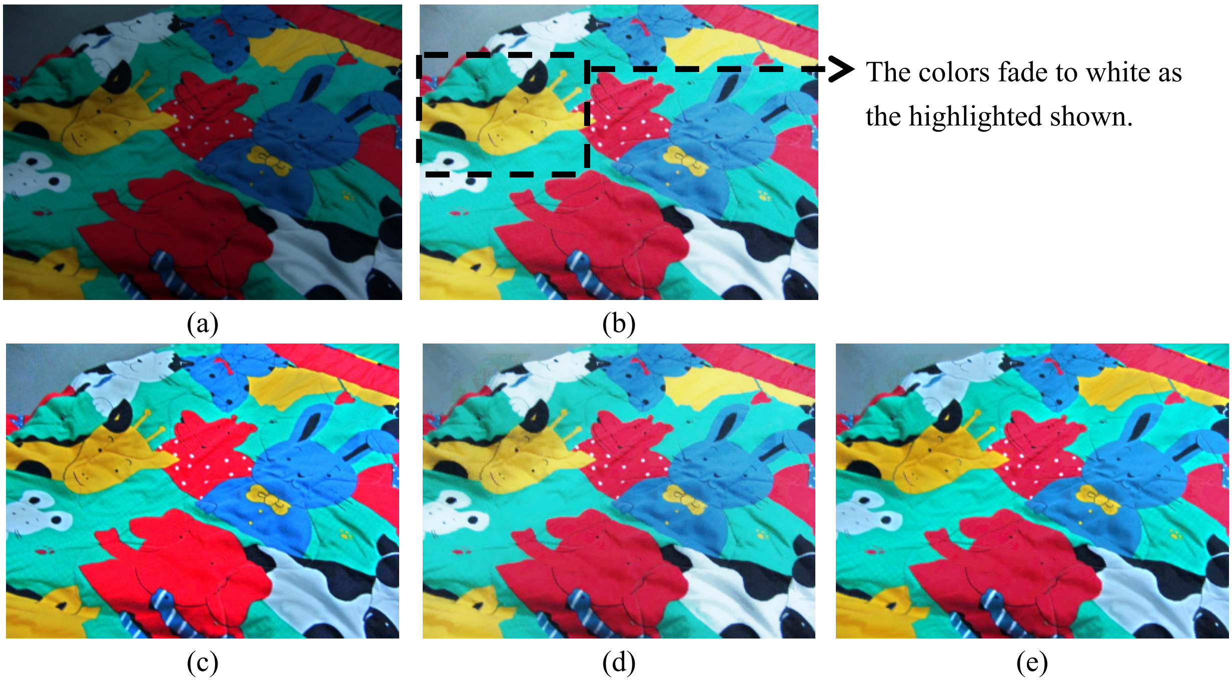

Fig. 23. LDR case. (a) Lowly-exposed input image I_L. (b) Highly-exposed input image I_H. (c) Local tone mapping result I_T. (d) Local color mapping result I_C. (e) Fusion result I_D.

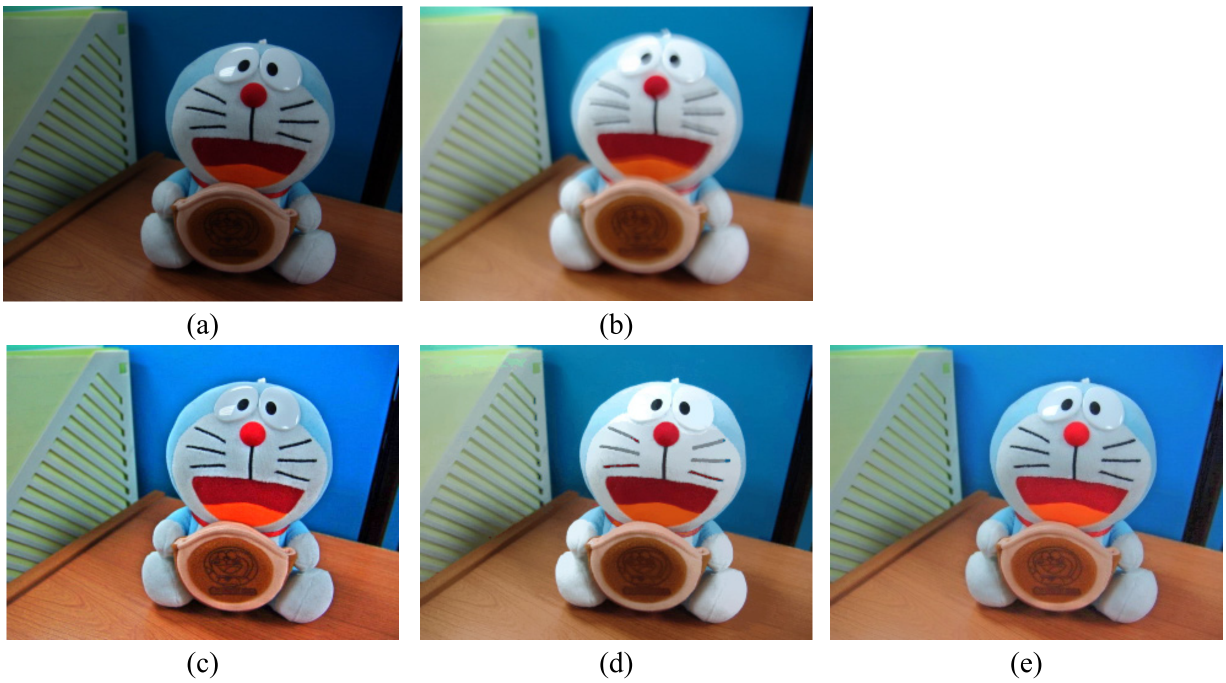

Fig. 24. Camera-shake case. (a) Lowly-exposed input image I_L. (b) Highly-exposed input image I_H. (c) Local tone mapping result I_T. (d) Local color mapping result I_C. (e) Fusion result I_D.

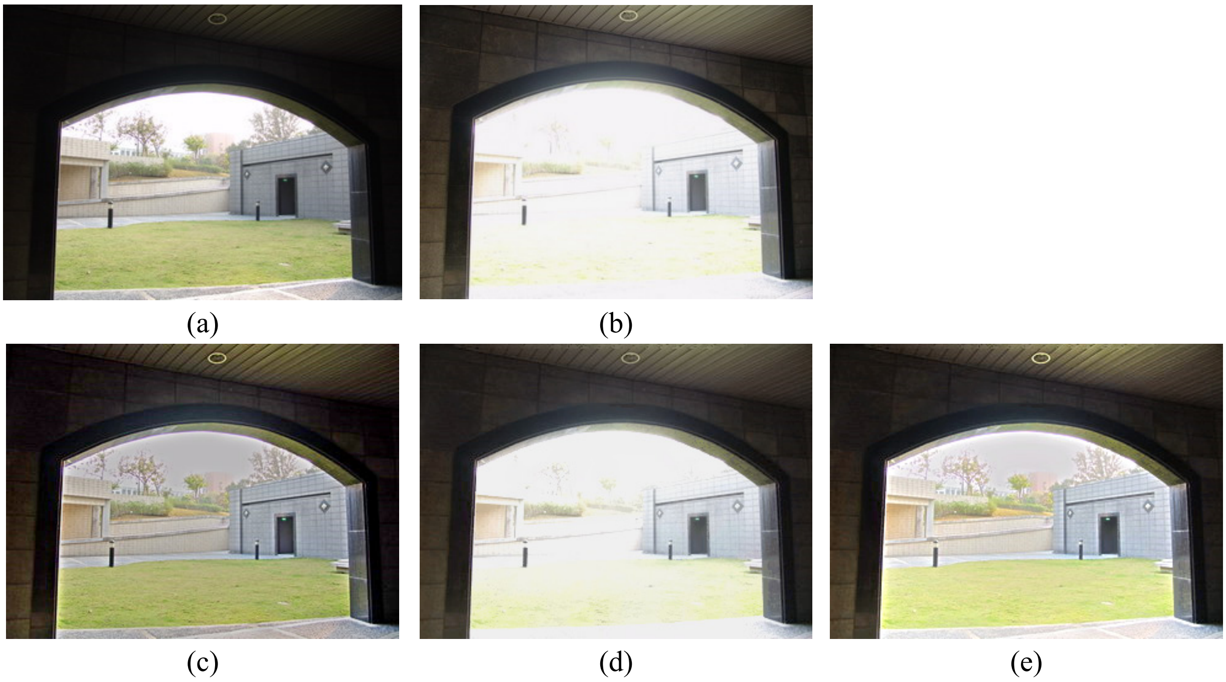

Fig. 25. Extreme HDR case. (a) Lowly-exposed input image I_L, (b) Highly-exposed input image I_H, (c) Local tone mapping result I_T, (d) Local color mapping result I_C, (e) Fusion result I_D.

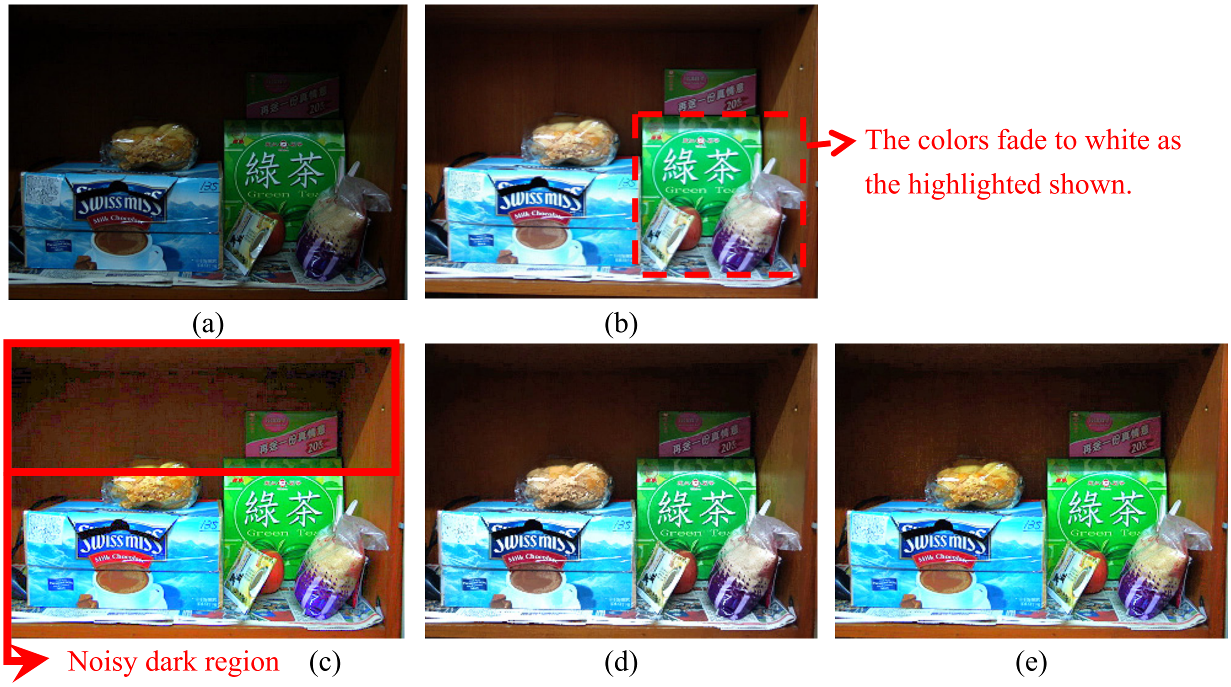

Fig. 26. Noise reduction case. Note that the red frames border the noisy dark regions of I_T. (a) Lowly-exposed input image I_L. (b) Highly-exposed input image I_H. (c) Local tone mapping result I_T. (d) Local color mapping result I_C. (e) Fusion result I_D.

TABLE I. ITEMIZED RUNNING TIME OF EACH PROCESS IN PROPOSED TONE REPRODUCTION SYSTEM WITHOUT USING MULTI-RESOLUTION APPROACH.

Process Item	Time (Seconds)
Local Region Determination	1.73
Local Tone Mapping Module	3.05
Local Color Mapping	2.41
Fusion Result	0.12
Total Time	7.31

TABLE II. OVERALL RUNNING TIMES OF PROPOSED TONE REPRODUCTION SYSTEM USING MULTI-RESOLUTION APPROACH WITH DIFFERENT LEVELS.

Level	0	1	2	3
Time (Seconds)	7.31	5.84	3.97	2.28

TABLE III. ITEMIZED RUNNING TIME OF EACH PROCESS IN PROPOSED TONE REPRODUCTION SYSTEM USING MULTI-RESOLUTION APPROACH WITH 3 LEVELS.

Process item	Time (Seconds)
Local Region Determination	0.65
Local Tone Mapping Module	0.79
Local Color Mapping	0.72
Fusion Result	0.12
Total Time	2.28